

# Chiral peptide nucleic acids having thymine and adenine in their side chain as specific ligands for Ni<sup>II</sup> and Cu<sup>II</sup>†

Justyna Brasuń,<sup>a</sup> Paola Ciapetti,<sup>b</sup> Henryk Kozłowski,<sup>\*a</sup> Stanisław Oldziej,<sup>c</sup> Maurizio Taddei,<sup>b</sup> Daniela Valensin,<sup>d</sup> Gianni Valensin<sup>d</sup> and Nicola Gaggelli<sup>d</sup>

<sup>a</sup> Faculty of Chemistry, University of Wrocław, F. Joliot-Curie 14, 50383 Wrocław, Poland.

E-mail: henrykoz@wchuwr.chem.uni.wroc.pl

<sup>b</sup> Dipartimento di Chimica, Università di Sassari, via Vienna 2, 07100 Sassari, Italy

<sup>c</sup> Faculty of Chemistry, University of Gdańsk, Sobieskiego 18, Gdańsk, Poland

<sup>d</sup> Dipartimento di Chimica, Università di Siena, 53100 Siena, Italy

Received 6th March 2000, Accepted 16th June 2000

Published on the Web 11th July 2000

Potentiometric and spectroscopic data, including NMR, CD and EPR results, as well as theoretical calculations showed that the insertion of a nucleic base into a peptide chain results in formation of very effective ligands (chiral peptide nucleic acids, C-PNAs) for Cu<sup>II</sup> and Ni<sup>II</sup>. The most effective ligand was that containing thymine base. The thymine moiety interacts with metal ion in the apical position *via* the O6 oxygen and forms a set of effective hydrogen bonds with the N-terminal amino group. In the case of adenine C-PNA, two nucleic bases may form stacking interactions, which also increases the complex stability. These interactions of nucleic bases mean that metal ion binding to peptide backbone nitrogens of PNAs leads to formation of complexes which are several orders of magnitude stronger than those obtained with oligoglycine. Metal ion binding to C-PNAs, on the other hand, induces specific conformations of the side chain groups, which would affect critically the self-recognition interactions between the C-PNA strands.

Peptide nucleic acids (PNAs) are synthetic analogues of DNA in which the natural phosphate–deoxyribose backbone is replaced with a peptide chain. Two types of PNA are known, one consisting of *N*-(aminoethyl)glycyl units<sup>1,2</sup> and another in which  $\alpha$ -amino acid residues carry DNA nucleobases in their side chains (chiral PNA, C-PNA).<sup>2,3</sup> The PNAs based on glycine are not chiral, and, as electrostatically neutral molecules, are capable of recognizing their complementary sequences in DNA and RNA.<sup>4</sup> They exhibit self-recognition similar to that of nucleic acid duplexes.<sup>2</sup> These latter PNAs are potentially capable of binding metal ions with both the peptide backbone donor system and the nucleobase donor set, while in achiral PNAs amide nitrogens are blocked and major binding sites are present in the nucleobases.

Our recent work on copper(II) co-ordination to a short C-PNA having thymine in the side chain position indicated

that the metal binding occurs at the peptide backbone, involving the N-terminal NH<sub>2</sub> and consecutive deprotonated amide nitrogens. The stability of the complexes formed is, however, several orders of magnitude higher than those of the respective complexes with simple oligoglycine peptides having the same binding mode.<sup>5</sup> This strongly suggests that nucleobases may stabilize very effectively metal complexes formed with C-PNAs even when not involved directly in the co-ordination. This stabilization may result, among others, from the interactions between different thymine rings. Thus, the metal ion bound to the peptide backbone may induce some specific organization of the thymines present in the C-PNA side chain.

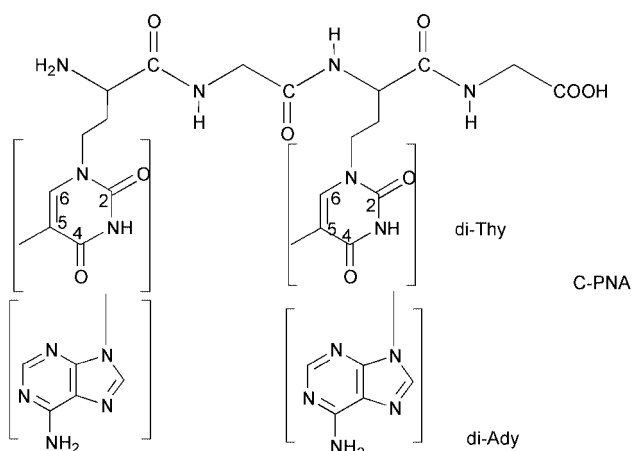
It should be mentioned that studies on the metal ion binding to monomeric amino acid–nucleobase analogues were developed earlier.<sup>6</sup> The coupling of an amino acid residue with a nucleic base yielded a very efficient ligand for metal ions.

In order to gain better understanding of the role of the thymine side chain in the stabilization of metal complexes with C-PNAs, we have extended our study on di-nucleobase C-PNA ligands and their complexes with Cu<sup>II</sup> and Ni<sup>II</sup>. To evaluate the interactions between thymines, theoretical calculations were also performed.

## Experimental

### Potentiometric measurements

Stability constants for proton, copper(II) and nickel(II) complexes were calculated from titration curves carried out at 25 °C using sample volumes of 1.5 cm<sup>3</sup>. Alkali was added from a 0.250 cm<sup>3</sup> micrometer syringe, which was calibrated by both weight titration and the titration of standard materials. The ligand concentration was 1 × 10<sup>−3</sup> mol dm<sup>−3</sup> and the metal-to-ligand ratios were 1 : 1 and 1 : 1.5. The pH-metric titrations were performed at 25 °C in 0.1 mol dm<sup>−3</sup> KNO<sub>3</sub> on a MOLSPIN pH-meter system using a Russel CMAW 711 semi-micro combined electrode calibrated in hydrogen ion concentrations using



† Electronic supplementary information (ESI) available: a colour version of Fig. 3. See <http://www.rsc.org/suppdata/doi/10.1039/b001763i>

HNO<sub>3</sub>.<sup>7</sup> Three titrations were performed for each molar ratio, and the SUPERQUAD computer program was used for stability constant calculations.<sup>8</sup> Standard deviations quoted were computed by SUPERQUAD, and refer to random errors only. They are, however, a good indication of the importance of a particular species in the equilibrium.

### Spectroscopic studies

Absorption spectra were recorded on a Beckman DU 650 spectrophotometer, circular dichroism (CD) spectra on a JASCO J 715-150 spectropolarimeter in the 850–250 nm range and EPR spectra on a Bruker ESP 300E spectrometer at X-band frequency (9.4 GHz) at 120 K. The metal concentration in these measurements was adjusted to  $1 \times 10^{-3}$  mol dm<sup>-3</sup> and metal to ligand ratios were 1:1. The spectroscopic parameters were obtained at the maximum concentration of the particular species as indicated by the potentiometric calculations.

### NMR studies

NMR experiments were carried out at 14.1 T (Bruker Avance 600) at controlled temperature ( $\pm 0.1$  K). Solutions were made in 99.95% deuterium oxide (Merck), adjusted in pH with either DCl or NaOD and carefully deoxygenated. <sup>1</sup>H and <sup>13</sup>C chemical shifts were referenced to internal [2H<sub>4</sub>]trimethylsilylpropane-sulfonate (TSP-d<sub>4</sub>).

The NMR spectra were obtained at pH 10.6 for the Ni<sup>II</sup>-di-Thy system (the complex with di-Ady was not soluble under these conditions) and ligand concentration of 6.86 mmol dm<sup>-3</sup>. A ligand-to-metal molar ratio 1:1 was used. NiCl<sub>2</sub> was the metal ion source.

Proton resonance assignment for ligand and complex was obtained by TOCSY, COSY and NOESY. TOCSY<sup>9</sup> experiments were acquired with a total spin-locking time of 75 ms using a MLEV-17 mixing sequence, NOESY<sup>10</sup> spectra with standard acquisition parameters and mixing times ranging from 300 to 500 ms. TOCSY and NOESY spectra were recorded in the phase-sensitive mode and with water suppression, COSY spectra in quantum filtered (QF) mode detection, without water suppression and using gradient pulses for selection.

Spin-lattice relaxation rates were measured with inversion recovery pulse sequences and calculated by exponential regression analysis of the recovery curves of longitudinal magnetization components.<sup>11</sup>

Heteronuclear (<sup>1</sup>H-<sup>13</sup>C) shift-correlated 2-D spectra (HMQC<sup>12,13</sup> and HMBC<sup>13</sup>) were obtained with standard pulse sequences, using gradient pulses for selection. The combined use of HMBC and HMQC (heteronuclear multiple bond and quantum correlation) facilitated the assignment of all carbon signals, particularly the non-protonated ones.

### C-PNA synthesis

The adenine and thymine oligomers were prepared using standard solid phase peptide chemistry following the Fmoc protocol in a batch manual synthesizer.<sup>14</sup> A Wang type resin loaded with Fmoc-Gly was used as the starting material. Fmoc deprotection was carried out using a 25% solution of piperidine in DMF. Coupling was carried out using benzotriazol-1-yloxy-tris(pyrrolidino)phosphonium hexafluorophosphate/*N,N*-diisopropylethylamine (PyBOP/DIPEA) in DMF for Fmoc-Gly and PyBOP/DIPEA in 1-methyl-2-pyrrolidone (NMP)-DMSO for the nucleobase containing Fmoc amino acids. With these compounds a double coupling was needed. The couplings and deprotections were monitored using the Kaiser test.<sup>15</sup> Oligopeptides were deprotected and cleaved from the resin using trifluoroacetic acid (TFA)-water (95:5). The products were precipitated from diethyl ether or acetone and dried under vacuum. HPLC analysis (Column C-18-Lichrospher 100, 5 µm, 250 × 4 mm, eluent MeCN-water (0.1% TFA) from 80:20 to 20:80 in 20 min, detector UV lamp,  $\lambda$  264 nm, flow 1 mL min<sup>-1</sup>)

**Table 1** Protonation constants of di-Thy, di-Ady and tetraGly at 25 °C and  $I = 0.1$  mol dm<sup>-3</sup> KNO<sub>3</sub>

Species	log $\beta$		
	di-Ady	di-Thy	tetraGly <sup>22</sup>
HL	6.72	10.29	7.97
H <sub>2</sub> L	10.92	19.92	11.15
H <sub>3</sub> L	14.34	26.48	—
H <sub>4</sub> L	17.14	28.51	—
pK <sub>1</sub> <sup>Ady(Thy)</sup>	4.20	10.29	—
pK <sub>2</sub> <sup>Ady(Thy)</sup>	3.42	9.63	—
pK(NH <sub>2</sub> )	6.72	6.56	7.97
pK(CO <sub>2</sub> <sup>-</sup> )	2.80	2.03	3.18

showed that the products were pure up to 90%. An analytical sample was isolated using preparative HPLC and submitted to ES-MS as previously described.<sup>14</sup> Results obtained in ES HRMS: for NH<sub>2</sub>Thy-Gly-Thy-GlyOH, C<sub>22</sub>H<sub>30</sub>N<sub>8</sub>O<sub>9</sub>, calc. *m/z* 568.2367, found 568.2401; for NH<sub>2</sub>Ady-Gly-Ady-Gly-OH, C<sub>22</sub>H<sub>28</sub>N<sub>14</sub>O<sub>5</sub>, calc. 550.2136, found 550.2126.

### Theoretical calculations

All *ab initio* calculations were carried out using a GAMESS 98 program.<sup>16</sup> The geometries of C-PNA complexes with metal ions were fully optimized at the restricted open-shell Hartree-Fock (ROHF) (for copper(II) complexes) or restricted Hartree-Fock (RHF) (for nickel(II)) level of theory. Owing to the system size we carried out all calculations using the Huzinaga MINI basis set.<sup>17</sup> Several possible structures of 4N complexes of C-PNAs and metal ions were built manually, although one can expect many more possible conformations due to the high flexibility of ethylene groups connecting the peptide backbone and nucleobases. The geometries of all structures were fully optimized and the nature of the stationary points was determined by analytical frequency calculations, verifying that they had no imaginary frequencies in the case of energy minima. A typical geometry optimization run took from five to eight days of computation time on a SGI Onyx (R12000 250MHz CPU) machine.

## Results and discussion

### Protonation constants

C-PNAs studied in this work consist of a dipeptide unit having thymine (Thy) or adenine (Ady) in the side chain of the first residue and the glycine residue in the second position, with general formula (X-Gly)<sub>*n*</sub> (X = Thy or Ady, *n* = 2). Four protonation constants calculated for the tetrapeptide ligand with NH<sub>3</sub><sup>+</sup>-Thy-Gly-Thy-Gly-OH sequence can be assigned to the carboxylate group (pK = 2.03), amino nitrogen (pK = 6.56) and two thymines (pK = 9.63 and 10.29, respectively) (Table 1).<sup>5</sup> The difference between the pK values of the two thymines is very close to the statistical value (0.66 vs. 0.6), suggesting no or negligible interaction between the two thymine rings in the metal free tetrapeptide. Also NH<sub>3</sub><sup>+</sup>-Ady-Gly-Ady-Gly exhibits four protonation constants assigned to carboxylate (2.80), amino (6.72) and two adenine nitrogens (3.42 and 4.20, respectively) (Table 1). The pK values of the two adenines differ by 0.78 indicating minor if any inter-ring interactions.

### Copper(II) complexes

The co-ordination modes for copper(II) complexes with a tetrapeptide having two thymines were described earlier.<sup>5</sup> Copper(II) ion co-ordinates to the C-PNA ligand in the same way as it binds to oligoglycine. The metal ion after anchoring at the N-terminal amino group co-ordinates to three consecutive deprotonated amide nitrogens forming 1N, 2N, 3N and 4N

**Table 2** Complex-formation constants of di-Thy, di-Ady and tetraGly at 25 °C and  $I = 0.1 \text{ mol dm}^{-3} \text{ KNO}_3$ 

	log $\beta$			log $K^*$		
	di-Ady	di-Thy	tetraGly <sup>22</sup>	di-Ady	di-Thy	tetraGly
CuH <sub>2</sub> L	—	24.98 (1N)	—	−2.46 (1N)	−1.5 (1N)	−2.90 (1N)
CuHL	—	19.91 (2N)	—	−7.30 (2N)	−6.57 (2N)	−8.51 (2N)
CuL	4.26 (1N)	14.61 (3N)	5.07 (1N)	−13.54 (3N)	−11.87 (3N)	−15.44 (3N)
CuH <sub>−1</sub> L	−0.58 (2N)	8.00 (4N)	−0.54 (2N)	−22.01 (4N)	−18.48 (4N)	−24.75 (4N)
CuH <sub>−2</sub> L	−6.82 (3N)	−0.1 (4N <sup>a</sup> )	−7.47 (3N)	—	—	—
CuH <sub>−3</sub> L	−15.29 (4N)	−10.68 (4N <sup>b</sup> )	−16.78 (4N)	—	—	—
pK <sub>1</sub> <sup>amide</sup>	4.84	5.07	5.61	—	—	—
pK <sub>2</sub> <sup>amide</sup>	6.24	5.30	6.93	—	—	—
pK <sub>3</sub> <sup>amide</sup>	8.47	6.61	9.31	—	—	—
pK <sub>1</sub> <sup>Thy(Ady)</sup>	—	8.10	—	—	—	—
pK <sub>2</sub> <sup>Thy(Ady)</sup>	—	10.58	—	—	—	—

	log $\beta$			log $K^*$		
	di-Ady	di-Thy	tetraGly <sup>23</sup>	di-Ady	di-Thy	tetraGly
NiL <sub>3</sub>	—	—	6.55	—	—	—
NiL	—	—	3.65 (1N)	—	—	−4.34 (1N)
NiH <sub>−1</sub> L	—	0.58 (4N)	−4.45 (2N)	—	—	−12.44 (2N)
NiH <sub>−2</sub> L	—	−8.87 (4N <sup>a</sup> )	−12.65 (3N)	—	—	−20.64 (3N)
NiH <sub>−3</sub> L	−19.48 (4N <sup>c</sup> )	−20.19 (4N <sup>b</sup> )	−20.90 (4N)	−26.20 (4N)	−25.90 (4N)	−28.89 (4N)
	−19.49 (4N <sup>d</sup> )	—	—	−26.21 (4N)	—	—
pK <sub>1</sub> <sup>amide</sup>	—	—	8.10	—	—	—
pK <sub>2</sub> <sup>amide</sup>	—	—	8.20	—	—	—
pK <sub>3</sub> <sup>amid</sup>	—	—	8.25	—	—	—
pK <sub>1</sub> <sup>Thy(Ady)</sup>	—	9.45	—	—	—	—
pK <sub>2</sub> <sup>Thy(Ady)</sup>	—	11.32	—	—	—	—

4N, 4N<sup>a</sup> and 4N<sup>b</sup> are complexes with four nitrogens and two, one and no thymine molecules protonated; 4N<sup>c</sup> is constant from potentiometric measurement and 4N<sup>d</sup> is constant from spectroscopic measurement.  $\log K^* = \log(\beta(\text{MH}_n\text{L})) - \log(\beta(\text{H}_n\text{L}))$ .

species, respectively. Thymines deprotonate above pH 8, thus the set of variously protonated 4N species is usually observed (Table 2, Fig. 1a). The spectroscopic and potentiometric data indicate that also the adenine ligand forms a similar set of complexes with copper(II) ions (Table 2, Fig. 1b). The pH dependence of the d–d transition energy and the  $\epsilon$  value (Table 3) allows us to assign the number of bound nitrogens in particular species.<sup>18</sup> There is no experimental indication that donors of thymine or adenine are involved in the strong direct interaction with Cu<sup>II</sup>. The potentiometric and spectroscopic data, however, show that the formation of the 4N species with the {NH<sub>2</sub>,3N<sup>−</sup>} co-ordination mode occurs at a considerably lower pH for thymine and adenine containing ligands than that with simple tetraglycine (Fig. 1). This co-ordination mode is realized above pH 8.5 for a simple oligopeptide, while in the systems studied here it happens above pH 5 for the di-thymine analogue<sup>5</sup> and above pH 7 for the di-adenine ligand (Fig. 1). Thus, the most effective ligand is that having two thymine side chains, while simple tetraglycine is the weakest ligand among the three collected in Table 2. This result strongly suggests the existence of interactions involving the two nucleobases within the ligand molecule, with thymines being the most effective (see below).

### Nickel(II) complexes

Both potentiometric and spectroscopic data show that nickel(II) yields three major species with the di-Thy ligand, NiH<sub>−1</sub>L, NiH<sub>−2</sub>L and NiH<sub>−3</sub>L all being square-planar 4N complexes (Fig. 2, Table 3). The first two species contain two and one protonated thymine, respectively. The pK value of 11.32 is higher than that of the “free” ligand (10.29, Tables 1,2). This may indicate the involvement of the thymine residue in the interactions (e.g. hydrogen bond formation) within the complex molecule. It is worthy to note that the pK values of thymine protonations in copper(II) complexes are considerably lower than those in nickel(II) 4N species (Table 2), suggesting different “stabilizing” interactions in the two types of complexes.

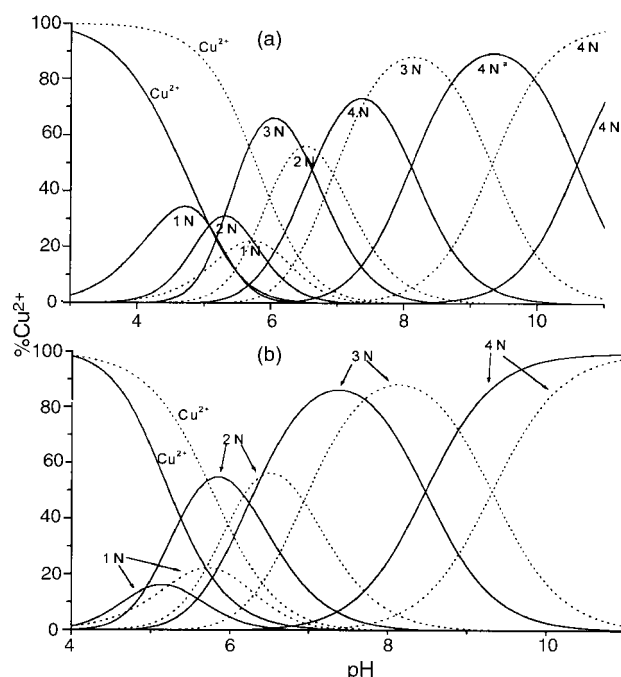


**Fig. 1** Species distribution curves for (a) Cu<sup>II</sup>–di-Thy (solid line) and Cu<sup>II</sup>–tetraGly (dotted line) solutions as a function of pH (the 4N, 4N<sup>a</sup> and 4N<sup>b</sup> species are the 4N complexes with two, one and no thymine protonated, respectively); (b) Cu<sup>II</sup>–di-Ady (solid line) and Cu<sup>II</sup>–tetraGly (dotted line) solutions as a function of pH. Ligand to metal molar ratio 1 : 1, ligand concentration  $1 \times 10^{-3} \text{ mol dm}^{-3}$ .

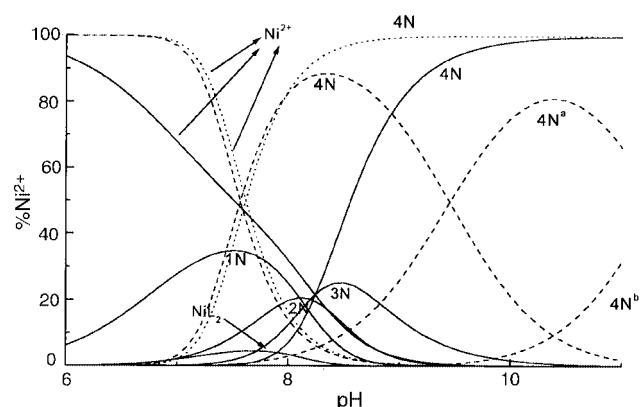
Very similar behavior is observed in the Ni<sup>II</sup>–di-Ady system. Potentiometric and spectroscopic data suggest formation of one major 4N square-planar complex. It is interesting that, contrary to Cu<sup>II</sup>, the stabilities of nickel(II) 4N complexes with both oligo-PNAs are very close to each other and distinctly higher than that obtained for tetraglycine.

**Table 3** Spectroscopic data for copper(II) and nickel(II) complexes of di-Thy and di-Ady

	di-Thy						di-Ady					
	UV-VIS		CD		EPR		UV-VIS		CD		EPR	
	$\lambda/\text{nm}$	$\epsilon/\text{M}^{-1}\text{cm}^{-1}$	$\lambda/\text{nm}$	$\Delta\epsilon/\text{M}^{-1}\text{cm}^{-1}$	$A_{\parallel}/G$	$g_{\parallel}$	$\lambda/\text{nm}$	$\epsilon/\text{M}^{-1}\text{cm}^{-1}$	$\lambda/\text{nm}$	$\Delta\epsilon/\text{M}^{-1}\text{cm}^{-1}$	$A_{\parallel}/G$	$g_{\parallel}$
CuHL	647 (2N)	55	—	—	—	—	—	—	—	—	—	—
CuL	570 (3N)	86	—	—	170	2.253	—	—	—	—	—	—
CuH <sub>1</sub> L	504 (4N)	127	552	−0.44	183	2.231	—	—	—	—	—	—
CuH <sub>2</sub> L	504 (4N)	131	539	−0.58	191	2.219	552 (3N)	112	—	—	—	—
CuH <sub>3</sub> L	505 (4N)	131	536	−0.63	196	2.181	505 (4N)	174	523	−0.34	210	2.167

	di-Thy				di-Ady			
	UV-VIS		CD		UV-VIS		CD	
	$\lambda/\text{nm}$	$\epsilon/\text{M}^{-1}\text{cm}^{-1}$	$\lambda/\text{nm}$	$\Delta\epsilon/\text{M}^{-1}\text{cm}^{-1}$	$\lambda/\text{nm}$	$\epsilon/\text{M}^{-1}\text{cm}^{-1}$	$\lambda/\text{nm}$	$\Delta\epsilon/\text{M}^{-1}\text{cm}^{-1}$
NiH <sub>1</sub> L	404 (4N)	80	453	−0.73	—	—	—	—
NiH <sub>2</sub> L	401 (4N)	127	458	−1.45	—	—	—	—
			399	−0.80				
NiH <sub>3</sub> L	401 (4N)	177	457	−1.38	405 (4N)	269	450	−1.07
			397	−0.17			416	−1.00

**Fig. 2** Species distribution curves for Ni<sup>II</sup>-di-Ady (dotted line), -di-Thy (dashed line) and -tetraGly (solid line). The 4N, 4N<sup>a</sup> and 4N<sup>b</sup> species are as in Fig. 1(a).

The variations of the chemical shifts of di-Thy upon nickel(II) co-ordination in the planar complex (Table 4) are very distinct and support the binding of metal ion to four consecutive nitrogens of the PNA ligand. The largest <sup>1</sup>H chemical shifts are observed for protons adjacent to the bound nitrogens, *i.e.* those bound to C<sub>α</sub> carbons, and of the <sup>13</sup>C chemical shifts for amide C=O and C<sub>α</sub> carbons. This result clearly indicates classical binding of Ni<sup>II</sup> to peptide backbone nitrogens. The co-ordination of metal ion to the PNA, however, has also distinct impact on the chemical shift of the ring carbons and C6 proton of N-terminal Thy (Table 4). The most striking changes are observed for three carbons, C2, C4 and C6 of the N-terminal Thy ring, and to a lesser extent for C2 and C4 of the second Thy ring. Also the shift of the C6 proton by −1.080 ppm seems unusual. The metal binding sites are too remote to cause such considerable changes of the chemical shifts of the ring protons and carbons. Thus, the thymine rings must interact with each other. It is interesting that two carbons C2 and C4 are shifted towards higher field, while C6 and its proton are shifted towards lower field. The chemical shift changes of the ring carbons and protons derive from the effect of the vicinal aromatic ring current. Therefore, the positions of the two thymine rings in the Ni<sup>II</sup>-di-Thy complex are not parallel to each other (as expected for rings interacting only by stacking) but rather twisted towards an edge-to-face position (two rings are perpendicular to each other), similarly to that yielded by the theoretical calculations (see Fig. 3a,b). The inter-ring

interactions also affect the C2 and C4 carbonyl carbons of the <sup>3</sup>Thy thymine ring, which, according to theoretical calculations are directed towards the <sup>1</sup>Thy ring (Fig. 3a). Both carbons are shifted towards higher field when compared to those of the metal-free ligand. It should be mentioned that the changes of the chemical shifts of the ring carbons and protons are influenced also by the hydrogen bonds involving ring carbonyls and heterocyclic nitrogens.

There is a very strong chemical shift change upon co-ordination of the carbon atom of the C-terminal carboxylate group (−6.16 ppm). This may indicate the involvement of this carboxylate in an effective hydrogen bond with the vicinal bound amino group (see below for the results of theoretical calculations).

### Theoretical calculations

Fig. 3(a) shows the lowest energy structure of the copper(II) complex with the Thy peptide. The central ion is surrounded by four nitrogens in an almost ideal plane. The fifth co-ordination site is occupied by the O6 oxygen atom from the thymine moiety located directly over the copper(II) ion. The Cu–O distance is 2.62 Å. The second thymine forms a hydrogen bond between the proton from the bound N-terminal amino group and the O2 oxygen of one of the thymine moieties. In some structures the formation of a hydrogen bond between the N3 hydrogen and the O2 oxygen atoms from two adjacent thymines is observed (see Fig. 3b). These structures, however, had slightly higher energy than the lowest energy structure shown in Fig. 3(a) (about 5–6 kcal mol<sup>−1</sup>). In all structures a very strong hydrogen bond formed between the proton from the N-terminal amino group and one of the oxygen atoms from the C-terminal carboxylate anion. The Cu–N distances observed for all structures investigated in our study vary from 1.799 to 1.820 Å. Such distances observed in structures of copper(II) complexes deposited in the CSDS<sup>19</sup> database vary from 1.821 to 2.121 Å. This comparison shows that the theoretical approach used in our study underestimates the donor–acceptor distances. To obtain the correct distances between the central ion and ligands the utilization of split-valence basis sets and polarization functions on non-hydrogen atoms is required.<sup>20</sup> In the case of the complexes formed between copper(II) ions and Ady peptides we found that the central ion and four bound nitrogen atoms are in very similar positions to those described for Thy peptide complexes. The Ady peptide can form many conformations with very similar energies. In none

**Table 4** The  $^1\text{H}$  and  $^{13}\text{C}$  NMR data for di-Thy and its nickel(II) complex (4N) at pH 10.6. Chemical shifts are given in ppm relative to TSP

		<sup>1</sup> H (δ)		
Proton		ligand	complex	Δδ*
<sup>1</sup> THY	Hα	3.495	3.766	−0.271
	Hβ	2.092	2.602	−0.51
		1.970	1.933	0.037
	Hγ	3.862	3.955	−0.093
		3.828	3.955	−0.127
	H <sub>ar</sub>	7.385	8.465	−1.08
Me	1.848	1.964	−0.116	
<sup>2</sup> GLY	Hα	3.950	3.373	0.577
		3.950	3.088	0.862
<sup>3</sup> THY	Hα	4.427	3.204	1.223
	Hβ	2.300	2.085	0.215
		2.092	1.941	0.151
	Hγ	3.918	3.990	−0.072
		3.747	3.873	−0.126
	H <sub>ar</sub>	7.319	7.504	−0.185
	Me	1.833	1.872	−0.039
<sup>4</sup> GLY	Hα	3.764	3.476	0.288
		3.714	2.931	0.783
		<sup>13</sup> C (δ)		
Carbon		ligand	complex	Δδ*
<sup>1</sup> THY	Cα	55.028	62.065	−7.037
	Cβ	36.301	30.413	5.888
	Cγ	48.273	47.970	0.303
	C6	145.32	147.307	−1.987
	Me	14.999	15.080	−0.081
	C2	160.400	157.73	2.67
	C4	178.58	173.104	5.476
	C5	113.79	???	—
	CO	180.33	180.791	−0.461
	<sup>2</sup> GLY	Cα	45.450	54.535
CO		174.319	181.756	−7.437
<sup>3</sup> THY	Cα	53.942	59.294	−5.352
	Cβ	32.849	34.818	−1.969
	Cγ	48.603	48.131	0.472
	C6	145.11	145.38	−0.27
	Me	14.999	14.945	0.054
	C2	160.40	159.49	0.91
	C4	176.58	175.42	1.16
	C5	113.66	???	—
CO	175.42	182.16	−6.74	
<sup>4</sup> GLY	Cα	46.24	51.263	−5.023
	CO <sub>2</sub>	179.15	185.31	−6.16

Δδ\* = δ<sub>ligand</sub> − δ<sub>complex</sub>

of them one can observe the specific interactions between adenine(s) and copper ions or between adenine(s) and the peptide backbone. One of the structures obtained is presented in Fig. 3(c). The reasons why the Ady peptide, in contrast to the Thy peptide, cannot interact directly with the metal ion is the size of the adenine moiety, longer than the thymine, as well as a repulsive interaction with the ethylene linker from the opposite side of the 4N plane. However, structures having two adenines stacked (at ring–ring distances 3.6–4.0 Å) within one complex molecule are also observed (Fig. 3d). This is a case of less usual cross stacking interactions observed in RNA structures.<sup>21</sup> This type of interaction could explain the stabilizing effect observed for the copper(II) di-Ady 4N complex.

Thus, the theoretical considerations presented above explain why the thymine ligand is much more effective in stabilizing the 4N copper(II) complex than simple tetraglycine or its adenine analogue.

In the case of complexes of Thy and Ady peptides with nickel(II) ion the structures observed are very similar to those obtained for copper(II) ion. However, some differences in

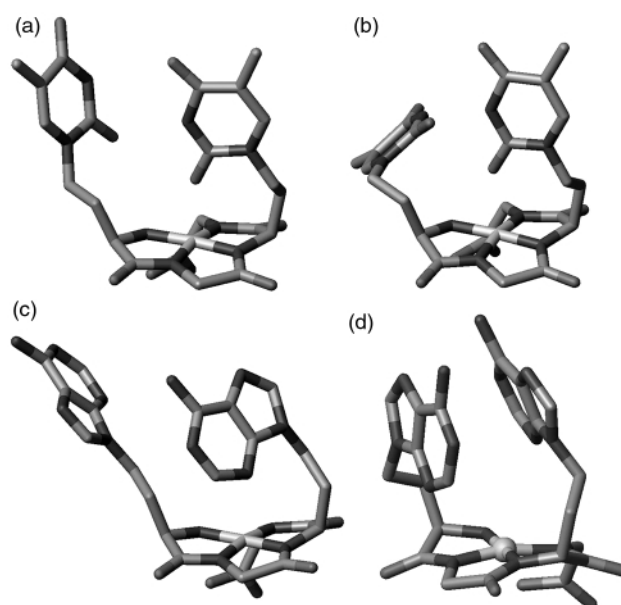


**Fig. 3** Calculated structures with di-Thy (a and b) and di-Ady (c and d). All hydrogen atoms are removed for clarity.

the geometry of interactions between the metal ions and the ligands are easily seen. The major difference between the 4N complexes with di-thymine PNA is in the apical interaction between the metal ion and the O6 of thymine. In the case of Ni<sup>II</sup> the oxygen–metal distance is distinctly longer (3.3–3.6 Å) when compared to that with Cu<sup>II</sup> (2.6 Å), in good agreement with the experimental data. The lack of stabilizing interactions in the apical position makes thymine and adenine ligands very similar to each other as was observed from the stability constants obtained for both ligands with nickel(II) ions. The proton and  $^{13}\text{C}$  NMR data discussed above strongly support the involvement of nucleic base rings in the interactions stabilizing metal–PNA complexes.

## Conclusion

Correlation of the stability constants obtained from the potentiometric and spectroscopic data, especially  $^1\text{H}$  and  $^{13}\text{C}$  NMR results, with theoretical calculations has shown that nucleic bases inserted into the peptide side chain in chiral peptide nucleic acids may stabilize the complex species in a quite significant manner. The formation of planar complexes with Cu<sup>II</sup> and Ni<sup>II</sup> allows thymine and adenine moieties to interact with the metal ion, the peptide backbone system or with an adjacent nucleic base to increase complex stability. The metal ion binding to C-PNAs, on the other hand, induces different types of interactions between the nucleic bases, critical for the organization of the side chains. The most important among them are the stacking interactions as well as the formation of hydrogen bonds between different base rings. These inter-base interactions can have a critical effect on the self-recognition between different C-PNA chains.

## Acknowledgements

This work was financially supported by Polish State Committee for Scientific Research and University of Wrocław. Calculations were carried out with the use of resources and software at the Informatic Centre of the Metropolitan Academic Network (IC TASK) at the Technical University of Gdańsk.

## References

- 1 P. E. Nielsen, M. Egholm, R. H. Berg and O. Buchardt, *Science*, 1991, **254**, 1497.
- 2 B. Falkiewicz, *Acta Biochim. Pol.*, 1999, **46**, 509.

- 3 A. Lenzi, G. Reginato, M. Taddei and E. Trifilieff, *Tetrahedron Lett.*, 1995, **36**, 1717.
- 4 M. Egholm, O. Buchardt, I. Christensen, C. Behrens, S. M. Freier, D. A. Driver, R. H. Berg, S. K. Kim, B. Nordén and P. E. Nielsen, *Nature (London)*, 1993, **365**, 566.
- 5 J. Szyrwił, P. Młynarz, H. Kozłowski and M. Taddei, *J. Chem. Soc., Dalton Trans.*, 1998, 1263.
- 6 K. Varnagy, M. Jeżowska-Bojczuk, J. Śwatek, H. Kozłowski, I. Sovago and R. W. Adamski, *J. Inorg. Biochem.*, 1990, **40**, 357 and references therein.
- 7 H. M. Irving, M. H. Miles and L. D. Pettit, *Anal. Chim. Acta*, 1967, **38**, 479.
- 8 P. Gans, A. Sabatini and A. Vacca, *J. Chem. Soc., Dalton Trans.*, 1985, 1196.
- 9 A. Bax and D. G. Davis, *J. Magn. Reson.*, 1985, **65**, 355.
- 10 M. Piotto, V. Saudek and V. Sklenar, *J. Biomol. NMR*, 1992, **2**, 661.
- 11 R. Freeman, H. D. W. Hill, B. L. Tomlinson and L. D. Hall, *J. Chem. Phys.*, 1974, **61**, 4466.
- 12 A. Bax and M. F. Summers, *J. Am. Chem. Soc.*, 1986, **108**, 4285.
- 13 L. Muller, *J. Am. Chem. Soc.*, 1979, **101**, 4481.
- 14 P. Ciapetti, A. Mann, A. Shoenfelder, I. Canet, M. Taddei and E. Trifilieff, *Lett. Peptide Sci.*, 1997, **4**, 341.
- 15 E. Kaiser, R. L. Colescott, C. D. Bosinger and P. I. Cook, *Anal. Biochem.*, 1970, **34**, 595.
- 16 M. W. Schmidt, K. K. Baldridge, J. A. Boatz, S. T. Elbert, M. S. Gordon, J. H. Jensen, S. Koseki, N. Matsunaga, K. A. Nguen, S. J. Su, T. L. Windus, M. Dupuis and J. A. Montgomery, *J. Comput. Chem.*, 1993, **14**, 1347.
- 17 S. Huzinaga, J. Andzelm, M. Klobukowski, E. Radzio-Andzelm, Y. Sakai and H. Tatewaki, *Gaussian basis sets for molecular calculations*, Elsevier, Amsterdam, 1984.
- 18 L. D. Pettit, J. E. Gregor and H. Kozłowski, in *Perspectives on Bioinorganic Chemistry*, eds. R. W. Hay, J. R. Dilworth and K. B. Nolan, JAI Press, London, 1991, p. 1 and refs. therein.
- 19 F. H. Allen, O. Kennar and R. Taylor, *Acc. Chem. Res.*, 1983, **16**, 146.
- 20 A. G. Baboul, P. C. Redfern, A. Sutjiano and L. Curtiss, *J. Am. Chem. Soc.*, 1999, **121**, 7220 and references therein.
- 21 Y. Li, G. Zon and W. D. Wilson, *Proc. Natl. Acad. Sci. U.S.A.*, 1991, **88**, 26.
- 22 W. Bal, H. Kozłowski, M. Lisowski, L. D. Pettit, R. Robbins and A. Safavi, *J. Inorg. Biochem.*, 1994, **55**, 41.
- 23 R. B. Martin, M. Chamberlin and J. T. Edsall, *J. Am. Chem. Soc.*, 1960, **82**, 495.